Performance of Initial Synchronization Schemes for W-CDMA Systems in Spatially Correlated Fading Channels

Lars Schmitt*, Thomas Grundler†, Christoph Schreyoegg‡, Gerd Ascheid*, and Heinrich Meyr*
*Institute for Integrated Signal Processing Systems
ISS, RWTH Aachen University, Germany
Email: {Schmitt, Ascheid, Meyr}@iss.rwth-aachen.de
†Siemens AG, Munich, Germany
Thomas.Grundler@siemens.com
‡Siemens AG, Ulm, Germany
Christoph.Schreyoegg@siemens.com

***Abstract*— Two different power-scaled noncoherent detection schemes are analyzed and compared in terms of detection probability and mean detection time in the uplink of a wideband CDMA system, where the mobile terminal transmits a pilot signal in the form of bursts of modulated chips, which are transmitted periodically and separated by long silent intervals. Both detection schemes employ temporal noncoherent averaging but differ in the way of spatial processing. One of the schemes, which is well suited for spatially uncorrelated scenarios, employs spatial noncoherent averaging, whereas the other scheme, better suited for scenarios with a distinct spatial structure, employs fixed beamforming. The performance analysis is carried out for spatially correlated frequency-selective fading channels taking channel dynamics and initial frequency offsets into account. With the presented analysis it is possible to investigate the effects of spatial correlation on the detection performance and to examine the improvement of using multiple antenna elements at the base station depending on the respective detection scheme.**

I. Introduction

In common DS-CDMA systems like UMTS [1], random access in the uplink is realized by means of a periodically transmitted pilot preamble. In particular, the terminal transmits bursts of known pilot chips separated by a long silent interval. After the pilot preamble has been detected by the base station, an acquisition indicator is sent back to the terminal and a dedicated communication link is established. The received preamble samples are also used for an initial timing acquisition of the channel taps. This initial timing information is passed on to the Rake structure [3], where it is used for processing the data symbols of the dedicated communication link and further refined using timing tracking structures as described in [2].

The detection of a known signal in a noisy environment is usually performed by means of binary hypothesis tests. Therefore, with a spacing of one chip period or a fraction of it, a region of the delay domain, the search window, is searched for the pilot signal. This search can either be done serially [4] or in parallel [5].

The binary tests are usually performed by correlating the received signal with the known pilot sequence and comparing the squared magnitude of the correlator output with a fixed threshold, see e.g. [6].

An important aspect is the impact of channel dynamics and an initial frequency offset. Due to the time-varying nature of the channel, not the whole pilot sequence may be used for coherent accumulation without undergoing degradation in performance. Hence, in order to exploit the temporal diversity of the fading channel, successive correlator outputs have to be accumulated noncoherently, as also proposed in [6].

The detection performance can be further improved by exploiting the spatial dimension through the use of multiple antenna elements at the base station receiver. Before initial acquisition occurs, parameters like the amplitudes and phases of the fading processes are not available and cannot be used for maximum ratio combining. Hence, it is straightforward to combine the antenna elements noncoherently as proposed in [7]. However, if the channel exhibits a distinct spatial structure, the concept of hypothesis tests in the delay domain can be extended to the spatial or angular domain, by performing a search over angular cells via directed beams, as proposed in [8].

Since the received interference level is unknown, some form of adaptive threshold setting is required to guarantee a constant false alarm rate (CFAR). Equivalently, the test statistic may be scaled by an estimate of the total received power as proposed in [9].

Thus, by jointly applying the concepts mentioned above, two basic decision schemes can be proposed to scan the search window for the pilot signal, which differ in the way of spatial processing. A block diagram of the scheme that employs spatial noncoherent averaging is depicted in Fig. 1(a). The scheme using fixed directional beams to search also the angular domain is illustrated in Fig. 1(b). Note, that the received power estimate used for scaling the test statistics is also based on the respective beam output, since the interference level may depend on the angular direction.

In [10] the analysis in terms of detection probability and mean detection time was carried out for the decision

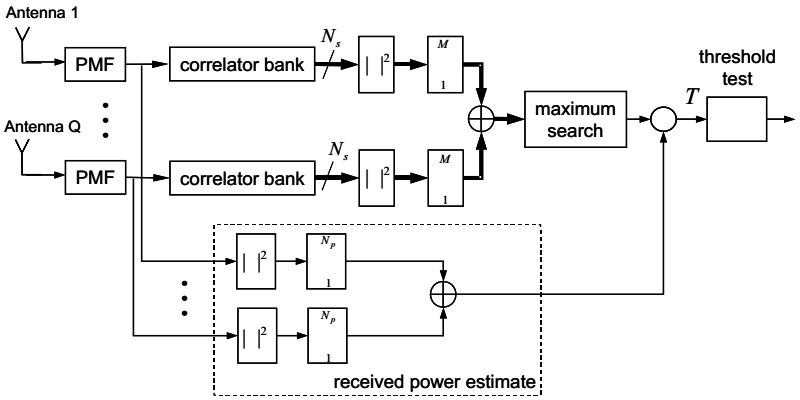

(a) Decision device employing spatial noncoherent averaging

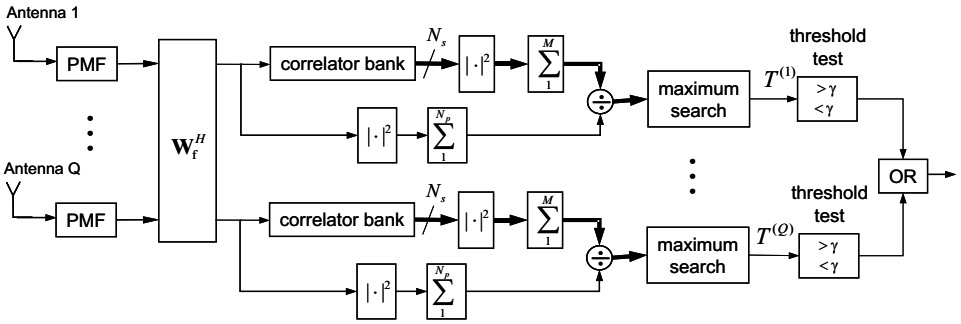

(b) Decision device employing spatial beamforming

Fig. 1. Block diagram of proposed power-scaled decision devices with temporal noncoherent averaging.

device in Fig. 1(a) for spatially uncorrelated scenarios. The focus of this paper is to extend the analysis to spatially correlated frequency selective Rayleigh fading channels for both proposed schemes and to compare their performance.

II. Received Signal Model

By employing Q antenna elements at the receiver, it is assumed that, due to the small size of the antenna array, the long-term channel statistics are identical at each antenna element.

The spatio-temporal multipath fading channel is modelled to consist of L dominant channel paths with non-zero variance σ_l^2 located at a delay τ_l with $l = 0, \ldots, L-1$. The total channel power is normalized to unity. Due to the WSSUS assumption the channel paths are assumed to be uncorrelated.

Assuming like in [5], that the receiver is chip synchronized with the user of interest and that the multipath delays $\tau_l = d_l T_c$ are integer multiples of the chip period T_c, the T_c-sampled version of the received signal after chip-matched filtering at the q-th antenna element can be written as

$$z_n^{(q)} = z^{(q)}(t = nT_c) = e^{j(2\pi f_e n T_c + \phi)} \sum_{l=0}^{L-1} h_{l,n}^{(q)} b_{n-d_l} + v_n^{(q)}, \tag{1}$$

for $n = 0, \ldots, N_p - 1$. The transmit and receive pulses are modelled within the effective channel coefficients $h_{l,n}^{(q)}$. The additive white Gaussian noise at each antenna element, which also models other user interference, is denoted by $v_n^{(q)}$ with variance σ_v^2, and b_n denotes the complex chips of a pilot burst of length N_p chips consisting of a periodically repeated signature scrambled by a long scrambling code like in [1]. A possible initial frequency and phase offset is denoted by f_e and ϕ, respectively.

The channel coefficients $h_{l,n}^{(q)}$ of the l-th channel path at the q-th antenna element are modelled as zero-mean complex Gaussian Rayleigh fading random processes with maximum Doppler frequency f_D. Let θ_l be the mean direction of arrival (DOA) of the l-th channel path and let the DOA be uniformly distributed over $[\theta_l - \delta_{\theta_l}, \theta_l + \delta_{\theta_l}]$, then, following Naguib [11] the correlation function of the channel coefficients may be expressed as

$$\mathrm{E}\{h_{l,k}^{(q)} h_{l,n}^{(p)^*}\} = \sigma_l^2 J_0(2\pi f_D [k-n] T_c) \boldsymbol{K}_{\mathrm{S},l}(q,p), \tag{2}$$

where J_0 denotes the zero-order Bessel function of first kind and $\boldsymbol{K}_{\mathrm{S},l}(q,p)$ denotes the element of the spatial correlation matrix $\boldsymbol{K}_{S,l}$ corresponding to the q-th row and p-th column and the l-th channel path

$$\boldsymbol{K}_{S,l} = \frac{1}{2\delta_{\theta_l}} \int_{\theta_l - \delta_{\theta_l}}^{\theta_l + \delta_{\theta_l}} \boldsymbol{a}(\theta) \boldsymbol{a}(\theta)^H \, d\theta. \tag{3}$$

For a uniform linear array with inter element spacing of $\Delta = 1/2$ wavelengths, the array response vector is

given by

$$\boldsymbol{a}(\theta) = [1, e^{2\pi\Delta\sin\theta}, \ldots, e^{2\pi(Q-1)\Delta\sin\theta}]. \quad (4)$$

Note, that the diagonal elements of $\boldsymbol{K}_{S,l}$ are unity.

III. Performance Analysis

In common DS-CDMA systems, like in UMTS [1], the possible starting points of the pilot bursts are known to the base station and hence, the total delay region of uncertainty can be constrained to N_s chips. The size N_s of the search window depends on the physical cell radius, which is usually in the range of up to several kilometers.
Due to the long silent interval it is assumed that the whole delay region of uncertainty is searched for a signal between two successive pilot bursts, i.e. a purely parallel search is performed.

A. Spatial Averaging Scheme

1) Test Statistic: The correlator bank in Fig. 1(a) consists of N_s sequence correlators, which partition the pilot sequence into $M = N_p/N_c$ nonoverlapping consecutive subsequences of length N_c and therefore, perform for each subsequence a coherent accumulation over N_c chips by correlating the received signal with the known pilot sequence corresponding to each tap within the search window. However, as mentioned above, due to the long silent interval between two successive pilot bursts it is not necessary to perform a completely parallel processing. The test statistic T (see Fig. 1(a)) can be written as

$$T = \max_{d\in\{0,\ldots,N_s-1\}} \frac{\sum_{q=0}^{Q-1}\sum_{m=0}^{M-1}\left|\boldsymbol{b}_d^{(m)H}\boldsymbol{z}^{(q,m)}\right|^2}{\sum_{q=0}^{Q-1}\sum_{n=0}^{MN_c-1}\left|z_n^{(q)}\right|^2}, \quad (5)$$

where $\boldsymbol{z}^{(q,m)} = [z_{mNc}^{(q)}, \ldots, z_{(m+1)Nc-1}^{(q)}]^T$ denotes the m-th received signal block at the q-th antenna element. The m-th block of the pilot sequence used for coherent accumulation with respect to a delay of d chips is denoted by $\boldsymbol{b}_d^{(m)} = [b_{mN_c-d}, \ldots, b_{(m+1)N_c-1-d}]^T$ setting $b_n = 0$ for $n < 0$ or $n > N_p - 1$. By defining the correlator output of the m-th signal block at antenna q corresponding to a delay d

$$x_d^{(q,m)} = \boldsymbol{b}_d^{(m)H}\boldsymbol{z}^{(q,m)}, \quad (6)$$

the numerator of the test statistic can be written as the noncoherent accumulation of the squared magnitude of the correlator outputs

$$T = \max_d \frac{\sum_{q=0}^{Q-1}\sum_{m=0}^{M-1}\left|x_d^{(q,m)}\right|^2}{\sum_{q=0}^{Q-1}\sum_{n=0}^{MN_c-1}\left|z_n^{(q)}\right|^2} = \max_d T_d. \quad (7)$$

2) Detection Probability: In this section an expression for the probability, that the test statistic T exceeds a certain threshold in case a pilot burst has been transmitted, is derived.
Since the received signal is zero-mean complex Gaussian distributed, the correlator outputs $x_d^{(q,m)}$ are also zero-mean jointly Gaussian distributed and completely characterized by their covariance.
By assuming good autocorrelation properties of the pilot scrambling sequence and using (2), the elements of the covariance matrix corresponding to the l-th channel path ($d = d_l$) can be easily calculated as follows

$$\begin{aligned}\mathrm{E}\{x_{d_l}^{(q,k)}x_{d_l}^{(p,n)*}\} =& \boldsymbol{K}_{\mathrm{S},l}(q,p)\boldsymbol{K}_{\mathrm{T},l}(k,n)\\ &+ N_c\sigma_v^2\delta(k-n)\delta(q-p),\end{aligned} \quad (8)$$

where $q,p = 0,\ldots,Q-1$ and $k,n = 0,\ldots,M-1$. The quantity $\delta(n)$ denotes the Kronecker-delta and the elements of the temporal correlation matrix $\boldsymbol{K}_{\mathrm{T},l}$ of the l-th channel path are given by

$$\begin{aligned}\boldsymbol{K}_{\mathrm{T},l}(k,n) = N_c\sigma_l^2 e^{j2\pi f_e N_c T_c(k-n)}&\sum_{u=-N_c+1}^{N_c-1}\left(1-\frac{|u|}{N_c}\right)\\ &\times J_0(2\pi f_D[N_c(k-n)+u]T_c)\cos(2\pi f_e u T_c).\end{aligned} \quad (9)$$

Note, if $d \notin \{d_0,\ldots,d_{L-1}\}$, the elements of the correlation matrix are just given by

$$\mathrm{E}\{x_d^{(q,k)}x_d^{(p,n)*}\} = N_c\sigma_v^2\delta(k-n)\delta(q-p). \quad (10)$$

Now, let all correlator outputs corresponding to a delay d be comprised in the vector

$$\boldsymbol{x}_d = [x_d^{(0,0)},\ldots,x_d^{(0,M-1)},\ldots,x_d^{(Q-1,0)},\ldots,x_d^{(Q-1,M-1)}]^T. \quad (11)$$

Then the total covariance matrix corresponding to the l-th channel path ($d = d_l$) is given by

$$\boldsymbol{K}_l = \mathrm{E}\{\boldsymbol{x}_{d_l}\boldsymbol{x}_{d_l}^H\} = \boldsymbol{K}_{\mathrm{S},l}\otimes\boldsymbol{K}_{\mathrm{T},l} + N_c\sigma_v^2\boldsymbol{I}_{QM} \quad (12)$$

where $\otimes$ denotes the Kronecker product, $\boldsymbol{I}_{QM}$ is the $(QM\times QM)$ identity matrix and $\boldsymbol{K}_{\mathrm{S},l}$ is the spatial correlation matrix from (2).
Thus, for $d \in \{d_0,\ldots,d_{L-1}\}$, the numerator of the test statistic T_d in (7) is the sum of the squared magnitude of MQ correlated complex Gaussian random variables, whereas for $d \notin \{d_0,\ldots,d_{L-1}\}$ the $x_d^{(q,m)}$ are independent.
The denominator in (7) is also a sum of chi-square distributed random variables, but due to the large number of degrees of freedom ($2QMN_c$) and since the chip signal-to-noise ratio $1/\sigma_v^2$ is very small it can be very well approximated by

$$\sum_{q=0}^{Q-1}\sum_{n=0}^{MN_c-1}\left|z_n^{(q)}\right|^2 \approx QMN_c(1+\sigma_v^2) \approx QMN_c\sigma_v^2. \quad (13)$$

Hence, T_d in (7) can be approximately written as

$$T_d \approx \frac{1}{QMN_c\sigma_v^2}\boldsymbol{x}_d^H\boldsymbol{x}_d. \tag{14}$$

The cumulative density function (cdf) of T_d in case a signal is present (hypothesis $\mathcal{H}_1$) is given by

$$F_{T_d|\mathcal{H}_1}(\gamma) = P\{T_d \le \gamma|\mathcal{H}_1\}. \tag{15}$$

A convenient way to calculate the cdf of T_d is by means of the characteristic function of T_d. According to [12], the characteristic function of the real quadratic form in (14) is given by

$$\Phi_{T_d|\mathcal{H}_1}(\omega) = \prod_{i=0}^{QM-1}\frac{1}{1-j\omega\lambda_d^{(i)}}, \tag{16}$$

for $d = d_l$, and the $\lambda_d^{(i)}$ are the eigenvalues of $\frac{1}{QMN_c\sigma_v^2}\boldsymbol{K}_l$. For $d \notin \{d_0,\dots,d_{L-1}\}$ the $\lambda_d^{(i)}$ are given by $1/QM$.

If all eigenvalues are distinct the pdf of T_d can be calculated via partial fractional expansion and inverse Fourier transformation of $\Phi_{T_d|\mathcal{H}_1}(\omega)$ in (16). Subsequently, the cdf is obtained from the pdf via integration. For distinct eigenvalues, one obtains (see e.g. [13])

$$F_{T_d|\mathcal{H}_1}(\gamma) = \sum_{i=0}^{QM-1} A_i e^{-\gamma/\lambda_d^{(i)}}, \tag{17}$$

with

$$A_i = \prod_{\substack{m=0\\m\neq i}}^{QM-1}\frac{1}{1-\frac{\lambda_d^{(m)}}{\lambda_d^{(i)}}}. \tag{18}$$

However, if the eigenvalues are not distinct as it is the case in spatially uncorrelated scenarios where in general M distinct Q-fold eigenvalues exists, it gets very complicated to obtain closed form solutions of the coefficients of the partial fractional expansion. Also, if the eigenvalues get very close to each other the calculation of the A_i in (18) gets numerically unstable. In these cases a numerically more stable way is to calculate the cdf of T_d directly via the characteristic function. According to the lemma of Gil-Pelaez (see e.g. [14]), the cdf $F_X(x)$ of a random variable X can be calculated via the characteristic function $\Phi_X(\omega)$ of X as follows

$$F_X(x) = \frac{1}{2} - \frac{1}{\pi}\int_0^\infty \frac{\mathrm{Im}\left\{\Phi_X(\omega)e^{-jx\omega}\right\}}{\omega}\,d\omega. \tag{19}$$

Therefore, the cdf of T_d can be expressed in terms of a single integral

$$\begin{aligned} F_{T_d|\mathcal{H}_1}(\gamma) &= \frac{1}{2} - \frac{1}{\pi}\int_0^\infty \frac{\mathrm{Im}\left\{\Phi_{T_d|\mathcal{H}_1}(\omega)e^{-j\gamma\omega}\right\}}{\omega}\,d\omega \\ &= \frac{1}{2} - \frac{1}{\pi}\int_0^\infty \mathrm{Im}\left\{\frac{e^{-j\gamma\omega}}{\omega\prod_{i=0}^{QM-1}(1-j\omega\lambda_d^{(i)})}\right\}d\omega, \end{aligned} \tag{20}$$

which can be evaluated numerically. Note, that the integrand is real valued and decays very fast for increasing ω. The limit of the integrand for $\omega \to 0$ exists and can easily be calculated

$$\lim_{\omega\to 0}\ \mathrm{Im}\left\{\frac{e^{-j\gamma\omega}}{\omega\prod_{i=0}^{QM-1}(1-j\omega\lambda_d^{(i)})}\right\} = -\gamma + \sum_{i=0}^{QM-1}\lambda_d^{(i)}. \tag{21}$$

Finally, with (17) or (20), respectively, the probability of detecting the pilot signal within the search window, and hence, achieving initial timing synchronization, can be calculated as

$$P_D = P\left\{\max_{d\in\{d_0,\dots,d_{L-1}\}} T_d > \gamma|\mathcal{H}_1\right\} \tag{22}$$

$$= 1 - P\left\{\bigcap_{d\in\{d_0,\dots,d_{L-1}\}} T_d \le \gamma|\mathcal{H}_1\right\} \tag{23}$$

$$= 1 - \prod_{d\in\{d_0,\dots,d_{L-1}\}} F_{T_d|\mathcal{H}_1}(\gamma), \tag{24}$$

where for the last equality the fact, that the events $T_d \le \gamma$ are independent, has been used.

3) False Alarm Probability: In case no signal is present (hypothesis $\mathcal{H}_0$), a false alarm event is very costly, since it results in the initiation of further signalling and processing procedures at the base station receiver. Hence, only a certain level of false alarm should be allowed.

Obviously, in case no signal is present, all correlator outputs $x_d^{(q,m)}$ are independently identically complex Gaussian distributed with zero-mean and variance $N_c\sigma_v^2$. Approximating the estimated received power by a constant, like in (13), the test statistic T_d can be expressed as the sum of the squared magnitude of QM uncorrelated complex identically distributed Gaussian random variables with variance $\frac{1}{QM}$, or equivalently, QMT_d is chi-square distributed with $2QM$ degrees of freedom.

Using the result for the right-tail probability of a chi-square distributed random variable with an even number of degrees of freedom (see e.g. [15]), the probability, that T_d exceeds a threshold γ in case no signal is present, is for all $d = 0,\dots,N_s-1$ given by

$$P\{T_d > \gamma|\mathcal{H}_0\} = e^{-QM\gamma}\sum_{k=0}^{QM-1}\frac{(QM\gamma)^k}{k!}. \tag{25}$$

The total probability of false alarm taking the search window of length N_s chips into account, is given by

$$P_F = P\left\{\max_{d\in\{0,\dots,N_s-1\}} T_d > \gamma|\mathcal{H}_0\right\} \tag{26}$$

$$= 1 - \left[1 - e^{-QM\gamma}\sum_{k=0}^{QM-1}\frac{(QM\gamma)^k}{k!}\right]^{N_s} \tag{27}$$

In order to calculate the value of the threshold corresponding to a specific false alarm probability, (27) has to be numerically solved for γ. Note, that the false alarm probability does not depend on the amount of interference σ_v^2, since the test statistic is scaled by the estimated total received power.

B. Spatial Beamforming Scheme

1) Test Statistic: For the spatial beamforming scheme in Fig. 1(b) the whole processing is performed within the beam domain. The proceeding in this section is analogous to Part A taking the different spatial processing into account. Note, that the beamforming operation can be implemented in the RF-part of the receiver by using an analog beamformer or by a digital beamformer in the baseband. According to each of the Q fixed beams the test statistics $T^{(q)}$ with $q = 0,\dots,Q-1$ can be written as

$$T^{(q)} = \max_{d\in\{0,\dots,N_s-1\}} \frac{\sum_{m=0}^{M-1}\left|\boldsymbol{b}_d^{(m)H}\boldsymbol{Z}^{(m)}\boldsymbol{w}^{(q)*}\right|^2}{\sum_{m=0}^{M-1}\left\|\boldsymbol{Z}^{(m)}\boldsymbol{w}^{(q)*}\right\|^2}, \tag{28}$$

where $\boldsymbol{Z}^{(m)} = [\boldsymbol{z}^{(0,m)},\dots,\boldsymbol{z}^{(Q-1,m)}]$ denotes the matrix which comprises the m-th received signal block of all antenna elements. The beamforming vector $\boldsymbol{w}^{(q)}$ is the q-th column of the beamforming matrix $\boldsymbol{W}_{\mathrm{f}}$. The beam vectors are assumed to be orthogonal (e.g. Butler matrix) in order to maintain spatially uncorrelated noise samples after beamforming, i.e. $\boldsymbol{w}^{(q)H}\boldsymbol{w}^{(p)} = \delta(q-p)$. Like in Part A, by defining the correlator output of the m-th signal block at beam q corresponding to a delay d

$$x_d^{(q,m)} = \boldsymbol{b}_d^{(m)H}\boldsymbol{Z}^{(m)}\boldsymbol{w}^{(q)*}, \tag{29}$$

the numerator of the test statistic can be written as the noncoherent accumulation of the squared magnitude of the correlator outputs

$$T^{(q)} = \max_d \frac{\sum_{m=0}^{M-1}\left|x_d^{(q,m)}\right|^2}{\sum_{m=0}^{M-1}\left\|\boldsymbol{Z}^{(m)}\boldsymbol{w}^{(q)*}\right\|^2} = \max_d T_d^{(q)}. \tag{30}$$

2) Detection Probability: Analogously to (8), it can easily be shown that the covariance between the correlator outputs corresponding to the l-th channel path is given by

$$\begin{aligned}\mathrm{E}\{x_{d_l}^{(q,k)}x_{d_l}^{(p,n)*}\} =& \boldsymbol{w}^{(q)H}\boldsymbol{K}_{\mathrm{S},l}\boldsymbol{w}^{(p)}\boldsymbol{K}_{\mathrm{T},l}(k,n)\\ &+ \boldsymbol{w}^{(q)H}\boldsymbol{w}^{(p)}N_c\sigma_v^2\delta(k-n)\\ =& \boldsymbol{w}^{(q)H}\boldsymbol{K}_{\mathrm{S},l}\boldsymbol{w}^{(p)}\boldsymbol{K}_{\mathrm{T},l}(k,n)\\ &+ N_c\sigma_v^2\delta(k-n)\delta(q-p),\end{aligned} \tag{31}$$

where the fact, that the beamforming vectors are mutually orthogonal, has been used. Note, if $d \notin \{d_0,\dots,d_{L-1}\}$, the elements of the correlation matrix are just given by

$$\mathrm{E}\{x_d^{(q,k)}x_d^{(p,n)*}\} = N_c\sigma_v^2\delta(k-n)\delta(q-p). \tag{32}$$

Using the definition for $\boldsymbol{x}_d$ in (11) the total covariance matrix corresponding to the l-th channel path ($d = d_l$) is given by

$$\begin{aligned}\boldsymbol{K}_l =& \mathrm{E}\{\boldsymbol{x}_{d_l}\boldsymbol{x}_{d_l}^H\}\\ =& \boldsymbol{W}_{\mathrm{f}}^H\boldsymbol{K}_{\mathrm{S},l}\boldsymbol{W}_{\mathrm{f}}\otimes\boldsymbol{K}_{\mathrm{T},l} + N_c\sigma_v^2\boldsymbol{I}_{QM}.\end{aligned} \tag{33}$$

With the same reasoning as in Part A, the denominator of the test statistic in (30) is approximated as a constant

$$\sum_{m=0}^{M-1}\left\|\boldsymbol{Z}^{(m)}\boldsymbol{w}^{(q)*}\right\|^2 \approx MN_c\sigma_v^2. \tag{34}$$

Hence, $T_d^{(q)}$ in (30) can be approximately written as

$$T_d^{(q)} \approx \tfrac{1}{MN_c\sigma_v^2}\boldsymbol{x}_d^{(q)H}\boldsymbol{x}_d^{(q)}. \tag{35}$$

Note, that the covariance matrix of $\boldsymbol{x}_d^{(q)}$ is given by extracting the corresponding sub-matrix in (33)

$$\begin{aligned}\boldsymbol{K}_l^{(q)} =& \mathrm{E}\{\boldsymbol{x}_{d_l}^{(q)}\boldsymbol{x}_{d_l}^{(q)H}\}\\ =& \left(\boldsymbol{w}^{(q)H}\boldsymbol{K}_{\mathrm{S},l}\boldsymbol{w}^{(q)}\right)\boldsymbol{K}_{\mathrm{T},l} + N_c\sigma_v^2\boldsymbol{I}_M.\end{aligned} \tag{36}$$

Hence, the characteristic function of $T_d^{(q)}$ in case a signal is present is given by

$$\Phi_{T_d^{(q)}|\mathcal{H}_1}(\omega) = \prod_{i=0}^{M-1}\frac{1}{1-j\omega\lambda_d^{(i)}}, \tag{37}$$

for $d = d_l$, and the $\lambda_d^{(i)}$ are the eigenvalues of $\frac{1}{MN_c\sigma_v^2}\boldsymbol{K}_l^{(q)}$. For $d \notin \{d_0,\dots,d_{L-1}\}$ the $\lambda_d^{(i)}$ are given by $1/M$.

Analogously to Part A, for distinct eigenvalues the cdf of $T_d^{(q)}$ is given by

$$F_{T_d^{(q)}|\mathcal{H}_1}(\gamma) = \sum_{i=0}^{M-1}A_i e^{-\gamma/\lambda_d^{(i)}}, \tag{38}$$

with

$$A_i = \prod_{\substack{m=0\\m\neq i}}^{M-1}\frac{1}{1-\frac{\lambda_d^{(m)}}{\lambda_d^{(i)}}}. \tag{39}$$

For closely spaced or multi-fold eigenvalues the cdf may be calculated via numerical integration

$$F_{T_d^{(q)}|\mathcal{H}_1}(\gamma) = \frac{1}{2} - \frac{1}{\pi}\int_0^\infty \mathrm{Im}\left\{\frac{e^{-j\gamma\omega}}{\omega\prod_{i=0}^{M-1}(1-j\omega\lambda_d^{(i)})}\right\}d\omega, \tag{40}$$

with the limit of the integrand for $\omega \to 0$

$$\lim_{\omega\to 0}\ \mathrm{Im}\left\{\frac{e^{-j\gamma\omega}}{\omega\prod_{i=0}^{M-1}(1-j\omega\lambda_d^{(i)})}\right\} = -\gamma + \sum_{i=0}^{M-1}\lambda_d^{(i)}. \tag{41}$$

Note, that compared to the spatial averaging scheme the size of the search window is increased by a factor of Q resulting in a size of N_sQ hypotheses for the spatial beamforming scheme. Hence, the probability of

detecting the pilot signal within the search window is given by

$$P_D = P\left\{\max_{d\in\{d_0,\ldots,d_{L-1}\}}\max_{q=0,\ldots,Q-1} T_d^{(q)} > \gamma|\mathcal{H}_1\right\}. \tag{42}$$

Unfortunately, in general for arbitrary DOA's θ_l and angular spreads δ_{θ_l}, the test statistics of different beams $T_d^{(q)}, T_d^{(p)}$ are not independent and hence, one can not proceed like in Part A. Therefore, the consideration is restricted to two special cases

a) *Spatially uncorrelated scenario:*
In a spatially uncorrelated scenario the spatial covariance matrix is the identity matrix $\boldsymbol{K}_{\mathrm{S},l} = \boldsymbol{I}_Q$. By noting that ${\boldsymbol{w}^{(q)}}^H \boldsymbol{I}_Q \boldsymbol{w}^{(p)} = \delta(q-p)$, the total covariance matrix of the correlator outputs becomes

$$\boldsymbol{K}_l = \boldsymbol{I}_Q \otimes \boldsymbol{K}_{\mathrm{T},l} + N_c\sigma_v^2 \boldsymbol{I}_{QM}. \tag{43}$$

Therefore, the correlator outputs corresponding to different beams $\boldsymbol{x}_d^{(q)}$, $\boldsymbol{x}_d^{(p)}$ are independent and thus, also the corresponding test statistics $T_d^{(q)}$, $T_d^{(p)}$. Now, (42) can be written as

$$\begin{aligned} P_D &= 1 - P\left\{\bigcap_{\substack{d\in\{d_0,\ldots,d_{L-1}\}\\ q=0,\ldots,Q-1}} T_d^{(q)} \le \gamma|\mathcal{H}_1\right\} \\ &= 1 - \prod_{\substack{d\in\{d_0,\ldots,d_{L-1}\}\\ q=0,\ldots,Q-1}} F_{T_d^{(q)}|\mathcal{H}_1}(\gamma). \end{aligned} \tag{44}$$

Furthermore, the $T_d^{(q)}$ are identically distributed for all $q = 0,\ldots,Q-1$. Hence, P_D can be written as

$$P_D = 1 - \prod_{d\in\{d_0,\ldots,d_{L-1}\}} \left(F_{T_d^{(q)}|\mathcal{H}_1}(\gamma)\right)^Q. \tag{45}$$

b) *Fully correlated scenario:*
In a spatially fully correlated scenario the angular spread is equal to zero ($\delta_{\theta_l} = 0$). Furthermore, if we consider a best case scenario, i.e. the direction of arrival θ_l of the l-th channel path is perfectly matched to the direction of one of the fixed beam vectors $\boldsymbol{w}^{(q_l)}$, it is ${\boldsymbol{w}^{(q_l)}}^H \boldsymbol{a}(\theta_l) = \sqrt{Q}$, and hence ${\boldsymbol{w}^{(q)}}^H \boldsymbol{K}_{\mathrm{S},l} \boldsymbol{w}^{(p)} = {\boldsymbol{w}^{(q)}}^H \boldsymbol{a}(\theta_l)\boldsymbol{a}^H(\theta_l)\boldsymbol{w}^{(p)} = Q\delta(q-p)\delta(q-q_l)$. Thus, the spatial covariance matrix of the correlator outputs gets

$$\boldsymbol{K}_l = Q\boldsymbol{i}_{q_l}\boldsymbol{i}_{q_l}^T \otimes \boldsymbol{K}_{\mathrm{T},l} + N_c\sigma_v^2\boldsymbol{I}_{QM}, \tag{46}$$

where $\boldsymbol{i}_{q_l}$ is the q_l-th column of $\boldsymbol{I}_Q$. Now, (42) can be written as

$$\begin{aligned} P_D &= 1 - P\left\{\bigcap_{d\in\{d_0,\ldots,d_{L-1}\}} T_d^{(q_l)} \le \gamma|\mathcal{H}_1\right\} \\ &= 1 - \prod_{d\in\{d_0,\ldots,d_{L-1}\}} F_{T_d^{(q_l)}|\mathcal{H}_1}(\gamma). \end{aligned} \tag{47}$$

3) False Alarm Probability: Since the beamforming vectors are mutually orthogonal, the test statistics $T_d^{(q)}$ are independent in case no signal is present. To be precise, $MT_d^{(q)}$ is chi-square distributed with 2M degrees of freedom. According to the fact, that the size of the search window is QN_s, the total probability of false alarm for the beamforming decision devise is

$$P_F = P\left\{\max_{\substack{d\in\{0,\ldots,N_s-1\}\\ q=0,\ldots,Q-1}} T_d^{(q)} > \gamma|\mathcal{H}_0\right\} \tag{48}$$

$$= 1 - \left[1 - e^{-M\gamma}\sum_{k=0}^{M-1}\frac{(M\gamma)^k}{k!}\right]^{QN_s} \tag{49}$$

C. Mean Detection Time

Let the mean detection time $\overline{T}_D$ be defined as the average time it takes to achieve initial synchronization in terms of detecting a random access event. Usually, like in [1] the pilot bursts are repeated with increasing power. Let ρ_0 be the chip-to-interference ratio of the initial pilot burst, which is incremented by $\Delta\rho$ after each transmission. Furthermore, let T_p denote the time between the starting points of two consecutively transmitted bursts and $T_{D_i} = iT_p$ the time it takes that the pilot sequence is detected after i successive transmissions, then the mean detection time can be calculated as follows

$$\begin{aligned} \overline{T}_D =& \mathrm{E}\{T_{D_i}\} \\ =& \sum_{i=1}^{\infty} iT_p \Pr\left\{\begin{matrix}\text{preamble first detected}\\ \text{at } i\text{-th transmission}\end{matrix}\right\} \\ =& \sum_{i=1}^{\infty} iT_p P_D(\rho_0 + (i\text{–}1)\Delta\rho) \\ & \times \prod_{k=1}^{i-1}(1\text{–}P_D(\rho_0 + (k\text{–}1)\Delta\rho)), \end{aligned} \tag{50}$$

where $P_D(\rho)$ is given by (24) or (42), respectively, corresponding to a chip-to-interference ratio of $\rho = 1/\sigma_v^2$. Of course, for the evaluation of $\overline{T}_D$, the sum does not have to be taken up to ∞, since the probability that a preamble has not been detected until the i-th retransmission vanishes very rapidly with increasing i.

IV. Results

Since the analytical approach presented here has been verified by means of CCSS[1] system simulations in [10], this section focusses solely on the evaluation of the analytical results using MATLAB.

According to [1] the procedure considered for initial access is as described in Part C of section III with the following parameter setup. If not stated otherwise, the chip-to-interference ratio E_c/I of the first transmitted preamble arriving at the base station receiver is set to $\rho_0 = -30$ dB, which is incremented by $\Delta\rho = 1$ dB after each transmission. According to [16] the duration of a pilot burst is $N_p = 4096$ chips and the duration

[1]CoCentric System Studio from Synopsys.

between two successive transmissions is $T_p = 15360$ chips or equivalently 4 ms, since the chip duration equals $T_c = 1/(3.84 \cdot 10^6)$ s.

The search window is constrained to $N_s = 200$ chips and the threshold γ is normalized such that, that the rate of false alarm equals $P_F = 0.001$ for both considered schemes. The orthogonal fixed beams are generated by employing a butler matrix.

At first, the improvement of employing multiple antenna elements depending on the amount of spatial correlation is investigated. For a flat fading channel with a maximum Doppler frequency corresponding to a terminal velocity of 60 km/h, the mean detection time is plotted versus the number of antenna elements in Fig. 2. As shown in [10], according to the length of the pilot burst and the moderate channel dynamic, the received signal can be coherently averaged over the whole duration of the pilot burst, i.e. the correlator length equals $N_c = 4096$ and the temporal noncoherent averaging length is $M = 1$.

The dashed lines represent the results of the spatial averaging scheme, whereas the solid lines correspond to the spatial beamforming scheme. The line with the square-markers represents the one antenna case, where both schemes are equivalent and the shaded areas indicate the time intervals where a pilot burst is transmitted.

For both schemes the results are obtained for a fully correlated scenario ($\delta_\theta = 0°$) and an uncorrelated scenario, whereas two cases are distinguished for the beamforming scheme, a *best* case and a *worst* case. In the best case the DOA of the channel paths matches exactly the direction of a fixed beam, whereas for the worst case, the DOA lies just in the middle between two fixed beams. Note that for the uncorrelated scenario, the performance of the beamforming scheme is independent of the DOA.

The results were obtained by evaluating the analytical results of the previous section. If the special cases in part B Section III, which assess the performance of the beamforming scheme, were not applicable, the detection probability was obtained by means of Monte-Carlo simulations (evaluation of (35) and applying the decision rule).

Obviously, using both schemes the mean detection time can be significantly lowered by employing multiple antenna elements in case of a spatially correlated scenario as well as in uncorrelated scenarios. As expected, the spatial averaging scheme outperforms the beamforming scheme in uncorrelated scenarios. But even in a fully correlated scenario, the averaging scheme performs better than the beamforming scheme in the worst case.

In Fig. 3 the mean detection time is plotted versus the angular spread ranging from a fully correlated scenario ($\delta_\theta = 0°$) up to a spatially uncorrelated scenario $\delta_\theta = 180°$. As expected, the smaller the spatial correlation, the better the performance of the averaging scheme and the poorer the performance of the beamforming scheme. But this decrease in performance is not monotonic. As expected, in the worst case scenario the performance of the beamforming scheme is improved if the angular spread is not too large. This is due to the fact, that the beams adjacent to the DOA gather more signal energy as the signal is spread in the angular domain.

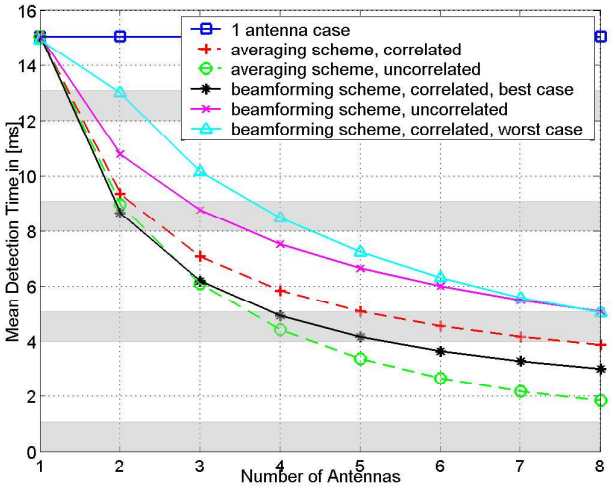

Fig. 2. Mean acquisition time versus the number of antenna elements, flat fading $v = 60$ km/h, $N_c = 4096, M = 1$.

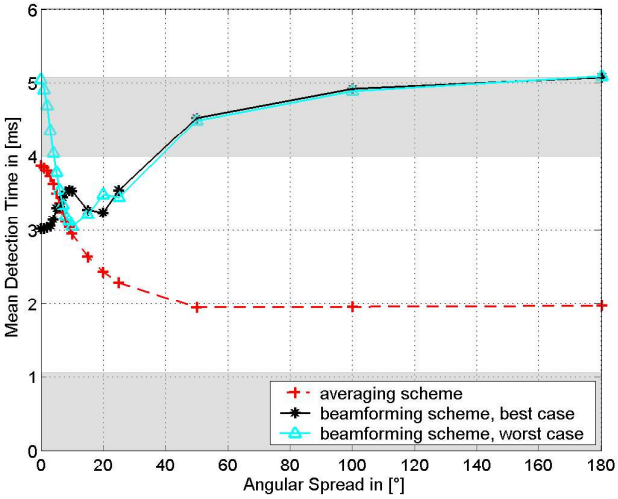

Fig. 3. Mean acquisition time versus angular spread, flat fading $v = 60$ km/h, $N_c = 4096, M = 1, Q = 8$ antenna elements.

Finally, the detection miss probability ($P_M = 1 - P_D$) is plotted versus the chip-to-interference ratio and the mean detection time is plotted versus the chip-to-interference ratio of the first arriving pilot burst in Fig. 4 and 5, respectively. The channel is frequency selective with four temporal taps located at delays of $\{0, 1, 2, 3\}$ chips with average tap powers $\{0, -3, -6, -9\}$ dB according to the Case 3 channel in the 3GPP standard with 60 km/h channel dynamics. From Fig. 4 it is apparent that a low detection miss probability especially for very low E_c/I is essential to achieve short acquisition times. In spatially fully correlated scenarios, the performance of the averaging

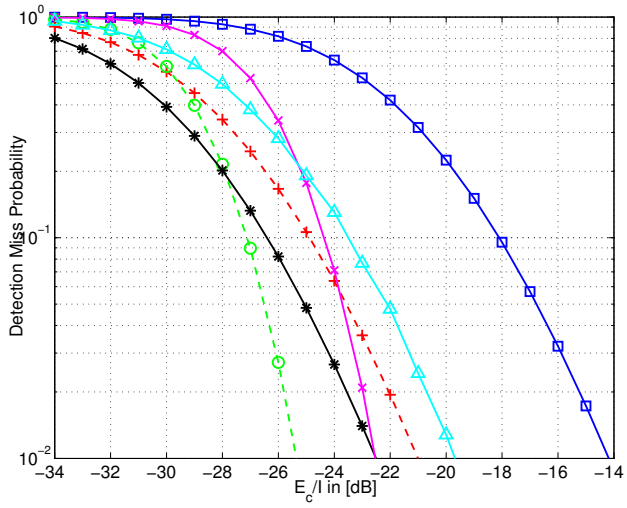

Fig. 4. Detection miss probability versus initial signal-to-noise ratio, Frequency selective channel (Case 3) $v = 60$ km/h, $N_c = 4096, M = 1, Q = 8$ antenna elements.

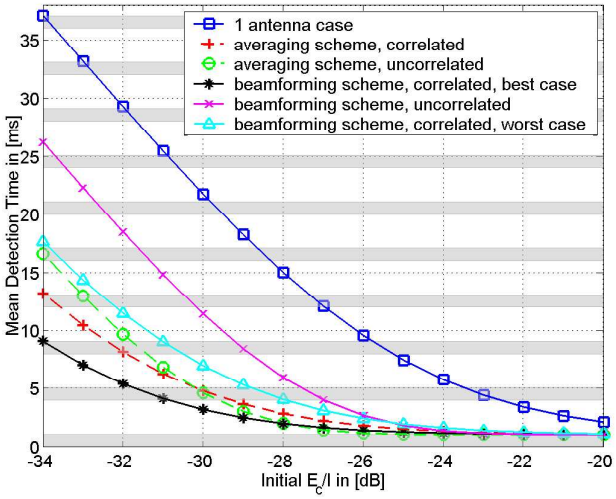

Fig. 5. Mean Acquisition time versus initial signal-to-noise ratio, Frequency selective channel (Case 3) $v = 60$ km/h, $N_c = 4096, M = 1, Q = 8$ antenna elemets.

scheme is within the performance range of the beamforming scheme with respect to the best and worst case. In uncorrelated scenarios, the averaging scheme clearly outperforms the beamforming scheme. Hence, for the system setup considered here, the use of a fixed beamforming scheme for initial synchronization can only be justified in correlated scenarios regarding the increased complexity.

V. Conclusion

An analytical framework for the performance in terms of detection probability and mean detection time of two power-scaled detectors using spatial averaging and spatial fixed beamforming, respectively, has been derived for the uplink of a W-CDMA system, where the initial synchronization is facilitated by the use of a periodically repeated pilot preamble. The performance analysis has been carried out for spatially correlated frequency selective fading channels taking an initial frequency offset and channel dynamics into account. It has been shown analytically, that the mean detection time can be significantly reduced by the use of multiple antenna elements even in scenarios with full spatial correlation. For the operating points considered in this paper the additional complexity of a detector with fixed beams can only be justified in correlated scenarios. The structure employing spatial averaging performs well in all considered scenarios and is not sensitive to the DOA and the amount of spatial correlation.

In correlated scenarios the performance of the beamforming scheme degrades mainly due to a significant loss in signal-to-noise ratio, which occurs if the direction-of-arrival of the channel path corresponds to the middle between two beam directions. Further investigations are in progress concerning spatial oversampling where more beams than antenna elements are applied in order to improve the detection performance in correlated scenarios.

References

[1] 3GPP TSG RAN. *Physical Layer Procedures (FDD)*, TS 25.214, June 2003.

[2] H. Meyr, M. Moeneclaey and S. Fechtel. *Digital Communication Receivers: Synchronization, Channel Estimation and Signal Processing*, John Wiley and Sons, New York, 1998.

[3] R. Price and P.E. Green Jr.. "A Communication Technique for Multipath Channels," *Proc. of the IRE*, Vol. 46, March 1958.

[4] A. Polydoros and C.L. Weber. "A Unified Approach to Serial Search Spread-Spectrum Code Acquisition - Part I: General Theory," *IEEE Trans. Commun.*, Vol, 32, No. 5, 542-549, Aug. 1977.

[5] R. Rick and L.B. Milstein. "Parallel Acquisition in Mobile DS-CDMA Systems," *Trans. Communications*, Vol. 45, No. 11, 1466-1476, November 1997.

[6] A.J. Viterbi. *CDMA Principles of Spread Spectrum Communication*, Reading, MA: Addison-Wesley, 1998.

[7] R. Rick and L.B. Milstein. "Parallel Acquisition of Spread-Spectrum Signals with Antenna Diversity," *IEEE Trans. Commun.*, Vol. 45, No. 8, 903-905, August 1997.

[8] M.D. Katz, J.J. Iinatti and S. Glisic. "Two-Dimensional Code Acquisition in Time and Angular Domains," *IEEE Trans. Commun.*, vol. 19, no. 12, pp. 2441-2451, December 2001.

[9] K. Choi, K. Cheun and T. Jung. "Adaptive PN Code Acquisition Using Instantaneous Power-Scaled Detection Threshold Under Rayleigh Fading and Pulsed Gaussian Noise Jamming," *IEEE Trans. Commun.*, vol. 50, no. 8, pp. 1232-1235, August 2002.

[10] L. Schmitt, V. Simon, T. Grundler, C. Schreyoegg and H. Meyr. "Initial Synchronization of W-CDMA Systems using a Power-Scaled Detector with Antenna Diversity in Frequency-Selective Rayleigh Fading Channels," accepted for *IEEE Global Commun. Conf. (Globecom)*, San Fransisco, USA, December 2003.

[11] A.F. Naguib. "Adaptive Antennas for CDMA Wireless Networks," Ph.D. dissertation, Stanford Univ., CA, August 1996.

[12] G.L. Turin. "The characteristic function of Hermitian quadratic forms in complex normal variables," *Biometrika*, 47:199-201, June 1960.

[13] R. Rick and L.B. Milstein. "Optimal Decision Strategies for Acquisition of Spread-Spectrum Signals in Frequency-Selective Fading Channels," *IEEE Trans. Commun.*, Vol. 46, No. 5, 686-694, May 1998.

[14] J. P. Imhof. Computing the distribution of quadratic forms in normal variables. *Biometrika*, vol. 48, nos. 3-4, pp. 419-426, 1961.

[15] S.M. Kay. *Fundamentals of Statistical Signal Processing - Detection Theory*, Prentice Hall, Upper Saddle River, NJ, 1998.

[16] 3GPP TSG RAN. *Physical Channels and Mapping of Transport Channels onto Physical Channels (FDD)*, TS 25.211, June 2003.